



# Geophysical Research Letters

## RESEARCH LETTER

10.1029/2019GL084332

### Key Points:

- We constrain the geothermal flux for three new locations beneath the Ross Ice Sheet
- Geothermal flux is near the global average for continental crust, in contrast to some previous estimates
- Existing characterizations of basal water and its effect on ice-flow are likely accurate

### Supporting Information:

- Supporting Information S1

### Correspondence to:

T. J. Fudge,  
tjfudge@uw.edu

### Citation:

Fudge, T. J., Biyani, S. C., Clemens-Sewall, D., & Hawley, R. L. (2019). Constraining geothermal flux at coastal domes of the Ross Ice Sheet, Antarctica. *Geophysical Research Letters*, 46, 13,090–13,098. <https://doi.org/10.1029/2019GL084332>

Received 28 JUN 2019

Accepted 27 SEP 2019

Accepted article online 22 OCT 2019

Published online 19 NOV 2019

## Constraining Geothermal Flux at Coastal Domes of the Ross Ice Sheet, Antarctica

**T. J. Fudge<sup>1</sup>, Surabhi C. Biyani<sup>1</sup>, David Clemens-Sewall<sup>2</sup>, and Robert L. Hawley<sup>2</sup>**

<sup>1</sup>Earth and Space Sciences, University of Washington, Seattle, WA, USA, <sup>2</sup>Earth Sciences, Dartmouth College, Hanover, NH, USA

**Abstract** The geothermal flux is an important boundary condition for ice-sheet models because it influences whether the ice is melting at the bed and able to slide. Point measurements and remotely sensed estimates vary widely for the Ross Ice Sheet. A basal temperature measurement at Roosevelt Island reveals a geothermal flux of  $84 \pm 13 \text{ mW/m}^2$ . The presence of Raymond Arches, which form only at ice divides that are frozen at the bed, allows inferences of the maximum geothermal flux at two coastal domes along the Siple Coast: Engelhardt Ridge,  $85 \pm 11 \text{ mW/m}^2$  and Shabtaie Ridge,  $75 \pm 10 \text{ mW/m}^2$ . These measurements indicate heat flows similar to measurements at Siple Dome and the Whillans grounding zone and to the continental crust average. The high values measured at Subglacial Lake Whillans and estimated from satellite observations of Curie depths are not widespread.

**Plain Language Summary** Heat flow from the earth helps determine whether an ice sheet can slide rapidly over the bed or is frozen to it. Few direct heat flow measurements exist because they require drilling through thousands of feet of ice. We present three new inferences of the heat flow for the Ross Ice Sheet in West Antarctica, approximately doubling the number of existing measurements. The heat flow is similar to the global average for continents and shows that previous inferences of higher heat flow are not widespread.

## 1. Introduction

The geothermal flux is an important basal boundary condition for ice-flow models (Golledge et al., 2014; Seroussi et al., 2017; Pollard et al., 2005). The geothermal flux affects whether the bed of the ice sheet is melting or frozen, and thus whether or not the ice sheet can slide. It also helps determine the rate of water that is either melting from or refreezing to the base of the ice sheet (Joughin et al., 2004; Joughin et al., 2009; Pollard et al., 2005). The geothermal flux is poorly constrained beneath ice sheets because direct observations are limited by needing to drill through hundreds to thousands of meters of ice. Interpretations of remotely sensed data are also limited by a lack of direct observations of the underlying geology (An et al., 2015; Fox Maule et al., 2005; Martos et al., 2017; Shapiro & Ritzwoller, 2004).

The geothermal flux, including beneath ice sheets, can vary significantly over distances of tens to hundreds of kilometers (Global Heat Flow Database, 2019). In central Greenland, the geothermal flux increases by a factor of 3 in the 300 km from Summit to NorthGRIP (Cuffey et al., 1995; Dahl-Jensen et al., 2003). In West Antarctica, significant spatial variability in the heat flux might be expected because much of the ice sheet overlies the West Antarctic Rift System (Behrendt et al., 1991; White-Gaynor et al., 2019) and there is significant volcanic activity (Van Wyk de Vries et al., 2018). Measurements of geothermal flux from direct observations are limited in West Antarctica (Figure 1). The value of  $69 \text{ mW/m}^2$  (Engelhardt, 2004) inferred at Siple Dome is similar to the average for continental crust ( $71 \text{ mW/m}^2$ , Davies & Davies, 2010). The Siple Dome value has been used to infer melt and refreezing rates for much of West Antarctica (Joughin et al., 2004; Joughin et al., 2009) yet whether it is representative of West Antarctica is unclear.

Measurements in the sediments beneath the Whillans grounding zone (Begeman et al., 2017) and subglacial lake Whillans (Fisher et al., 2015) revealed a transition from  $88 \pm 7 \text{ mW/m}^2$  to  $285 \pm 80 \text{ mW/m}^2$  in 100 km. The remotely sensed estimates (Figure 1) do not show any values nearly as high as at Subglacial Lake Whillans, but they still differ by a factor of 2, such as at the Byrd ice-core site, where Martos et al. (2017) infer  $136 \pm 22 \text{ mW/m}^2$  using satellite-measured Curie depths and An et al. (2015) find  $68 \text{ mW/m}^2$  using seismic

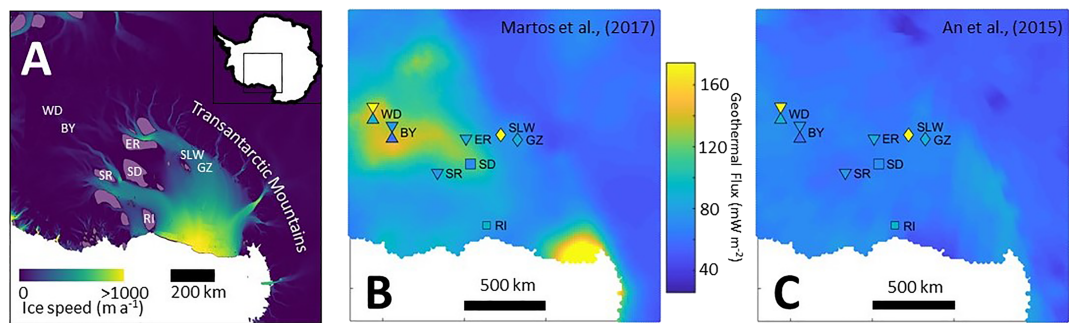


**Figure 1.** Ross sector of the West Antarctic ice sheet. (a) Ice flow velocities (Rignot et al., 2011) with purple masks indicating coastal domes (ice rises; Matsuoka et al., 2015). (b and c) Remotely sensed estimates of geothermal flux with direct inferences at individual locations. Down triangles are maximum estimates. Squares are values from ice-core sites with measured basal temperatures below freezing. Up and down triangles indicate upper and lower ends of range discussed in text. Diamonds are measurements in subglacial sediments (Begeman et al., 2017; Fisher et al., 2015). SD = Siple Dome; ER = Engelhardt Ridge; SR = Shabtaie Ridge; RI = Roosevelt Island; WD = West Antarctic ice sheet divide ice core; BY = Byrd ice core; SLW = subglacial Lake Whillans; GZ = grounding zone.

wave speeds. Thus, the geothermal flux beneath the Ross sector of the West Antarctic ice sheet remains uncertain.

We report three new constraints on the geothermal flux beneath the Ross Ice Sheet and reassess the geothermal flux at two interior ice-core sites, Byrd and WAIS Divide. The primary focus is using an ice-and-heat flow model in locations known to be frozen to the bed to constrain the geothermal flux. This builds on work by Siegert and Dowdeswell (1996) who used the presence of subglacial lakes to infer minimum geothermal flux values and the idea of a critical geothermal flux that determined the frozen/melting transition of Begeman et al. (2017). The first new constraint comes from Roosevelt Island where the basal ice temperature was measured as part of the Roosevelt Island Climate Evolution project (Bertler et al., 2018). The other two constraints use the observed Raymond Arches as an indication of a frozen bed; thus, the maximum geothermal flux can be inferred.

## 2. Data and Methods

### 2.1. Roosevelt Island Basal Temperature

We measured a basal temperature of  $-4.3^{\circ}\text{C}$  at Roosevelt Island in austral summers of 2013 and 2014 using a digital temperature probe with thin-film platinum resistance elements (Barry Narod, personal communication). No change in the basal temperature between 2013 and 2014 indicates that any drilling disturbance had dissipated. We calibrated the probe to an accuracy of within  $0.1^{\circ}\text{C}$  both before and after the field measurements at the United States Geological Survey temperature calibration facility in Boulder, Colorado. Additional details of the temperature measurements are in supporting information Text S1.

### 2.2. Temperature Modeling for sites with Raymond Arches

#### 2.2.1. Modeling Approach

An upward arch in internal layers beneath stable ice divides was predicted by Raymond (1983). The constitutive relation for ice is nonlinear (Glen, 1953), and the low deviatoric stress at a divide causes the ice to be stiffer. We refer to the different ice deformation pattern beneath a divide compared to the flank of an ice sheet as the Raymond effect. Raymond Arches have subsequently been found beneath many ice divides around Antarctica (Conway et al., 1999; Matsuoka et al., 2015; Vaughan et al., 1999). For a Raymond Arch to form beneath a divide, the divide needs to be: (1) stable for hundreds of years (i.e., stable for  $>1/10$  of the characteristic timescale defined as the ice thickness divided by the accumulation rate) and (2) frozen to the bed such that the Raymond effect operates.

The assumption made in this paper is that Raymond Arches are an indication that the bed is frozen, and there is no sliding. This assumption relies on two lines of evidence. The first is from model studies of ice divides. Pettit et al. (2003) showed that a linear sliding relation significantly reduces the Raymond effect. Martín et al. (2009) confirmed the linear sliding results in a full Stokes model. They also found that

nonlinear sliding relations with exponents less than the exponent in Glen's Flow Law ( $m < 3$ ) dampedened the Raymond Arch although at higher exponents and differing sliding fluxes the impact was more complicated. Thus it is likely, but not certain, that sliding will inhibit the formation of a Raymond Arch. The second line of evidence comes from observations. In every instance where an ice core has been drilled where a Raymond Arch was imaged, the bed has been frozen. These four sites are Siple Dome (Engelhardt, 2004; MacGregor et al., 2007), Berkner Island (Mulvaney et al., 2014), Fletcher Promontory (Mulvaney et al., 2014), and Roosevelt Island (this study). We also note that the Raymond effect was directly measured at Summit Greenland (Gillet-Chaulet et al., 2011) where the bed is frozen (Cuffey et al., 1995); however, no Raymond effect was observed at the NEEM ice-core site in Northwest Greenland where the bed is at the pressure-melting point (NEEM, 2013) although along-ridge flow may also be responsible for diminishing the Raymond effect.

### 2.2.2. Numerical Model

We use a one-dimensional, finite-volume, ice and heat flow model to calculate the ice-sheet temperature profile through time (Aydin et al., 2014; similar to Cuffey et al., 1995). The model domain includes 200 volumes in the ice and an additional 15 volumes extending 9 km into the bedrock where the geothermal flux is specified. We neglect horizontal temperature gradients and horizontal advection because these are small at ice divides. We thus solve:

$$\rho c \frac{\partial T}{\partial t} = \frac{\partial}{\partial z} \left[ k \frac{\partial T}{\partial z} \right] + \rho c w \frac{\partial T}{\partial z} + \dot{S} \quad (1)$$

Where  $T$  is temperature,  $t$  is time,  $z$  is vertical coordinate increasing from the bed toward the ice surface,  $\rho$  is density,  $c$  and  $k$  are temperature-dependent heat capacity and thermal conductivity (from Cuffey & Paterson, 2010, p. 400) for the ice and constant values for rock ( $750 \text{ J kg}^{-1} \text{ K}^{-1}$  and  $2.8 \text{ W m}^{-1} \text{ K}^{-1}$ ),  $w$  is the vertical velocity, and  $\dot{S}$  are the source terms (heating from vertical strain).

The model is run for 20 ka with a time step of 10 years. The model needs four primary forcings: the surface temperature history, the accumulation rate history, the vertical velocity profile, and the geothermal flux. The climate histories are approximated by a linear change from glacial to interglacial conditions from 18 to 12 ka. The base forcing has the temperature 10 °C colder and the accumulation rate 50% lower for the glacial compared to the Holocene. We also prescribe thinning of 20% of the present ice thickness between 18 and 12 ka for all domes based on the ice thickness history inferred for Siple Dome (Price et al., 2007; Waddington et al., 2005). The initial condition is a steady-state solution for the forcing at 20 ka. The vertical velocity profile uses the formulation of Lliboutry (1979):

$$w(\zeta) = w_s \left( 1 - \frac{p+2}{p+1} \zeta + \frac{1}{p+1} \zeta^{p+2} \right) \quad (2)$$

Where the vertical velocity profile,  $w$ , at normalized depth,  $\zeta$ , is parameterized using a shape factor,  $p$ , and the vertical velocity at the surface,  $w_s$ . The Lliboutry parameterization allows the influence of an ice divide on the vertical velocity profile to be represented by varying  $p$ . For Siple Dome, Engelhardt Ridge, and Shabtaie Ridge, we use  $p = -0.2$  for divide flow based on fitting the vertical velocity profile inferred from strain measurements below the summit of Siple Dome (Elsberg et al., 2004). For Roosevelt Island, we use  $p = -0.78$  for divide flow based on phase sensitive radar measurements (pRES, Kingslake et al., 2014). For all four sites, we use  $p = 4$  for flank flow based on the Roosevelt Island pRES measurements. Strain measurements at 500 m from the summit of Siple Dome and still within the area of the imaged Raymond Arch, show a transitional value of  $p = 2$ ; no strain measurements were made at Siple Dome outside area impacted by the Raymond effect. The Raymond Arch at each site indicates a different history of divide flow (Conway et al., 1999; Nereson & Raymond, 2001) and we vary  $p$  through time to represent the influence of the divide position. The histories of  $p$  used for the vertical velocity profile history for each site are shown in Figure S3 and are described below for each site (sections 3.1–3.4).

The geothermal flux is specified at the deepest node, 9 km into the bedrock, sufficiently deep that temporal variations in the ice temperature do not impact the boundary condition. The geothermal flux value is found by starting with a low value and increasing in  $1 \text{ mW/m}^2$  increments until the first instance of basal melt,

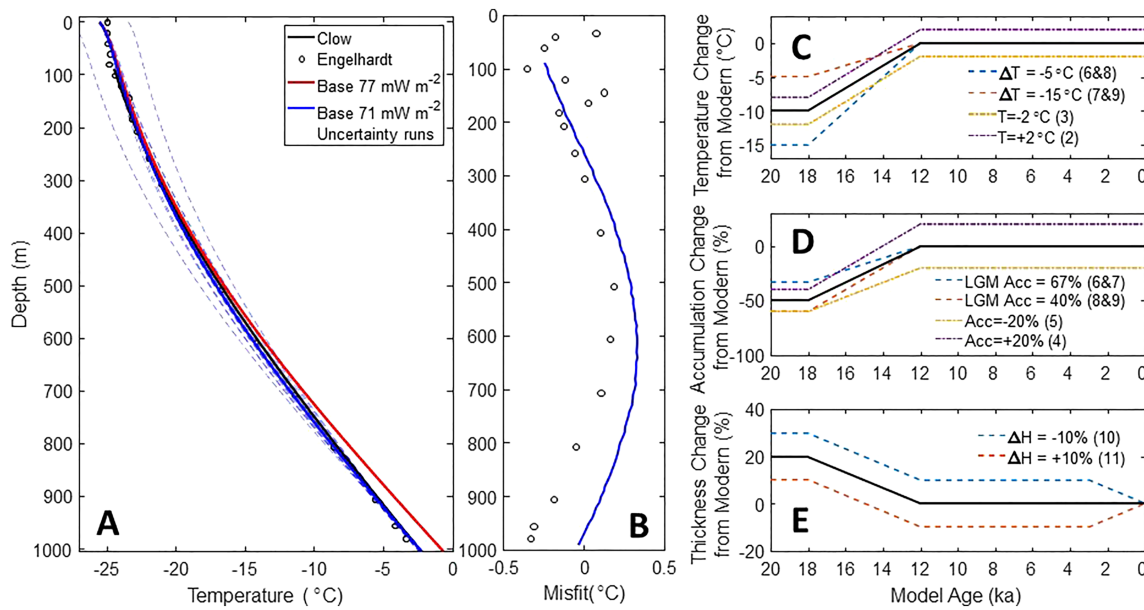


**Figure 2.** (a) Borehole temperature profiles for Siple Dome. Measurements shown in black (Clow in MacGregor et al., 2007; solid line; Engelhardt, 2004, circles). Model results with base forcing for measured basal temperature in blue and melting point red. All borehole temperature profiles of uncertainty runs are in dashed blue. (b) Misfit of base run with Engelhardt (circles) and Clow (solid blue) with no misfit in upper 100 m because the Clow measurements do not continue into the firn above the fluid-filled borehole. (c, d, and e) Model forcings for uncertainty runs. Black lines are base run (1).

which would violate the inference of a frozen bed where a Raymond Arch exists, or exceedance of the measured basal temperature. In all runs, the basal temperature increases throughout the Holocene such that the first instance of melt or basal temperature exceedance is at present, indicating that the basal temperature has always been colder than present.

### 2.2.3. Uncertainty Calculation

The uncertainty in the inferred geothermal flux is evaluated by varying the input parameters systematically. The base forcing (Run 1) is varied in five different ways (run numbers correspond to those of Figure 2 and Table S1):

1. Varying the modern surface temperature by  $\pm 2^\circ\text{C}$  (Runs 2 and 3)
2. Varying the modern accumulation rate by  $\pm 20\%$  (Runs 4 and 5)
3. Using  $5^\circ\text{C}$  and  $15^\circ\text{C}$  LGM-Holocene temperature change combined with glacial accumulation rates of 40% and 67% of modern (150% and 50% increases from glacial to modern; Runs 6–9)
4. Thicken or thin ice by 10% in past 3 ka (Runs 10 and 11)
5. Full divide flow or full flank flow for all time (Runs 12 and 13)

To compute the uncertainty, we first average each of the five sets of uncertainty runs and then combine them in quadrature. For the Engelhardt and Shabtaie Ridges, the uncertainty applies only to the inferred maximum geothermal flux and does not imply any constraint on the minimum geothermal flux. We discuss the relative magnitude of these uncertainty runs in section 3.1.

## 3. Results

### 3.1. Siple Dome

Siple Dome has been investigated previously, and an ice core has been drilled to bedrock (Nereson et al., 1998; Engelhardt et al., 2004; Taylor et al., 2004). Borehole temperatures have been measured with thermistor strings frozen into the ice column (Engelhardt, 2004) and in the fluid-filled ice-core borehole (Gary Clow, reported in MacGregor et al., 2007). Both show a basal temperature of  $-2.5^\circ\text{C}$ . Engelhardt inferred a geothermal flux of  $69 \text{ mW/m}^2$  using an ice flow model and method similar to what is described here. We use Siple Dome to illustrate our method and demonstrate that the model forcing produces a reasonable fit to the measured temperature profile.

We use a modern surface temperature of  $-25.5^{\circ}\text{C}$  (Engelhardt, 2004, S1), accumulation rate ( $0.13 \text{ m/a}$  ice eq., Hamilton, 2002), and ice thickness of  $1,004 \text{ m}$  (Taylor et al., 2004). Nereson et al. (1998) inferred divide migration at a rate between  $0.05$  to  $0.5 \text{ m/a}$ . We use a midvalue ( $0.25 \text{ m/a}$ ), which implies  $1 \text{ km}$  of migration in the past  $4 \text{ ka}$ . As the influence of divide flow is approximately one ice thickness,  $1 \text{ km}$  at Siple Dome, this suggests that the influence of divide flow at the present divide position began at  $4 \text{ ka}$ . We linearly change from  $p = 4$  at  $4 \text{ ka}$  to  $p = -0.2$  at present. We recognize this is a simplification for which we evaluate the uncertainty with the full flank and full divide uncertainty runs (12 and 13).

The borehole temperature measurements at Siple Dome are shown in Figure 2. We tested our model forcing by comparing the final modeled temperature profile with the measured one. The base forcing provides a good fit to the measurements with a maximum misfit of  $0.33^{\circ}\text{C}$  ( $\text{RMS} = 0.22^{\circ}\text{C}$ ). We find a geothermal flux of  $71 \text{ mW/m}^2$ , similar to the  $69 \text{ mW/m}^2$  inferred by Engelhardt (2004). The slight difference results from a higher accumulation rate, different vertical velocity profile history, and a different timing and magnitude of glacial climate change in the model forcings. Figure 2 also shows the modeled temperature profiles if the bed is assumed to be at the pressure melting point. We would infer a maximum geothermal flux of  $77 \text{ mW/m}^2$  for the base forcing, only  $6 \text{ mW/m}^2$  greater than when constrained by the basal temperature because the bed is already near the pressure melting point.

The temperature profiles and forcings of the 12 uncertainty runs are shown in Figure 2, and the differences in the inferred geothermal flux are shown in Table S1. We highlight a few implications. First, the  $\pm 2^{\circ}\text{C}$  surface temperature runs (2–3) affect the inferred geothermal flux nearly twice as much as the  $\pm 20\%$  accumulation runs (4–5). Second, glacial forcing runs (6–9) indicate that the temperature profile of Siple Dome could still be responding to the glacial climate. The largest impact is a  $10 \text{ mW/m}^2$  greater value for the  $15^{\circ}\text{C}$  colder and  $50\%$  reduction in accumulation. This forcing seems unlikely given that temperature and accumulation scale with each other on long timescales (Frieler et al., 2015), but we cannot reject it because the relationship is more complex at coastal sites (Fudge et al., 2016; Van Ommen et al., 2004). Third, the details of the vertical velocity profile do not significantly impact the inferred maximum geothermal flux; the full divide flow or full flank flow runs (12–13) result in no more than a  $6 \text{ mW/m}^2$  difference. This analysis likely overestimates the uncertainty for Siple Dome because some forcings can be excluded (e.g., the  $\pm 2^{\circ}\text{C}$  runs), but we retain these uncertainty runs because the other sites do not have measured temperature profiles.

### 3.2. Shabtaie Ridge

The glaciological characteristics of Shabtaie Ridge are very similar to Siple Dome and we use the same accumulation rate and an ice thickness of  $1,000 \text{ m}$  (Nereson et al., 2001). We use a  $0.5^{\circ}\text{C}$  warmer surface temperature because the summit is about  $50 \text{ m}$  lower and Shabtaie Ridge is located slightly to the north. Nereson et al. (2001) found that the Raymond Arch is wider than expected for a stable divide and inferred an oscillating divide position. Therefore, we use a forcing of that is in between divide and flank flow ( $p = 1$ , Figure S2), since the vertical velocity would primarily be transitional between flank and divide for the past  $2 \text{ ka}$  with the establishment of the divide occurring between  $3$  and  $2 \text{ ka}$ . Uncertainty run (12) uses full divide flow ( $p = -0.2$ ) for all times. The maximum geothermal flux is  $75 \pm 10 \text{ mW/m}^2$ .

### 3.3. Engelhardt Ridge

We use the same surface temperature as at Siple Dome assuming that the  $50\text{-m}$  lower surface elevation is offset by the more southerly position. We also use the same accumulation rate and vertical velocity profiles as at Siple Dome and an ice thickness of  $850 \text{ m}$  (Nereson et al., 2001). The imaged Raymond Arch is offset by  $5 \text{ km}$  from the modern divide, implying a recent (past  $\sim 1,000$  year) migration (Nereson et al., 2001). The base scenario uses a vertical velocity forcing where the divide became established between  $4$  and  $3 \text{ ka}$ ; full divide flow occurred between  $3$  and  $2 \text{ ka}$  before transitioning back to flank flow by  $1 \text{ ka}$ . We assume flank flow for the past  $1 \text{ ka}$  as the divide has migrated away. Uncertainty run (12) uses full divide flow ( $p = -0.2$ ) for all times. The inferred maximum geothermal flux is  $85 \pm 11 \text{ mW/m}^2$ .

### 3.4. Roosevelt Island

Extensive radar investigations were performed at Roosevelt Island (Conway et al., 1999; Kingslake et al., 2014) and a deep ice core was collected (Bertler et al., 2018). We use a modern surface temperature of  $-24$

°C, ice thickness of 765 m (Bertler et al., 2018), and accumulation rate of 0.22 m/a ice eq. (Winstrup et al., 2019). The onset of divide flow occurs between 4 and 3 ka (Conwat et al., 1999; Martín et al., 2006; Winstrup et al., 2019). The geothermal flux at Roosevelt Island is  $84 \pm 13 \text{ mW/m}^2$  using the basal temperature constraint of  $-4.3^\circ\text{C}$ . If no basal temperature had been measured, the inference of maximum geothermal flux would have been  $95 \text{ mW/m}^2$ .

## 4. Discussion

### 4.1. Siple Coast

The three new constraints on the geothermal flux (Table 1) are similar to two other measurements:  $71 \pm 10 \text{ mW/m}^2$  at Siple Dome and  $88 \pm 7 \text{ mW/m}^2$  at the Whillans grounding zone (Begeman et al., 2017). None of the values approach that of  $285 \pm 80 \text{ mW/m}^2$  inferred for Subglacial Lake Whillans (Fisher et al., 2015). The bulk of the measurements suggest a range of  $70\text{--}90 \text{ mW/m}^2$ , which are slightly higher than the global continental average of  $71 \text{ mW/m}^2$  (Davies & Davies, 2010), but similar to the Basin and Range in the Western USA ( $82\text{--}92 \text{ mW/m}^2$ , Lachenbruch et al., 1994), a geologic analog for the West Antarctic Rift System (Behrendt et al., 1991).

The remotely sensed estimates differ markedly from each other in Ross sector of West Antarctica (Figures 1b and 1c). Martos et al. (2017; hereafter M17) find a strong transition from high heat flow in the interior to low heat flow near the Transantarctic Mountains while the An et al. (2015; hereafter A15) values are lower and more uniform. The A15 values are lower than, and thus consistent with, the maximum constraints from Engelhardt and Shabtaie Ridges, in good agreement at Siple Dome and too low at the grounding zone and Roosevelt Island. The M17 values exceed the constraints at Siple Dome, Engelhardt Ridge, and Shabtaie Ridge (although Shabtaie Ridge is within the combined uncertainty), while the grounding zone measurement exceeds the M17 value (although again within the combined uncertainty). Therefore, the constraints do not support the spatial pattern of M17. Siple Dome, Engelhardt Ridge, and Shabtaie Ridge all lie on the edge of the M17 high flow region and additional constraints from central WAIS are needed to further assess the highest heat flows in the interior.

### 4.2. Interior Ross Ice Sheet

To assess the accuracy of the remotely sensed estimates in the interior (Figures 1b and 1c; M17; A15), we revisit the interpretation of the two deep ice-cores, Byrd (Gow et al., 1968) and WAIS Divide (WDPM, 2013), because there is confusion regarding the value and uncertainty of geothermal flux inferences for each site.

#### 4.2.1. Byrd Ice Core

When drilling at Byrd reached the bed, water entered the borehole indicating that the bed was at the pressure melting point. Using temperature measurements to a depth of 1,800 m, Gow et al. (1968) found a heat flux in the basal ice of  $75 \text{ mW/m}^2$ . This value has been interpreted as the geothermal flux (e.g., M17 Table S2); however, Rose (1979) inferred a geothermal flux of  $60 \text{ mW/m}^2$  by subtracting  $15 \text{ mW/m}^2$  of frictional heating from the 12 m/a velocity. This estimate did not assess the 4.8 m of accreted basal ice (Gow & Meese, 1996) nor the possibility of hydraulic supercooling as water flows uphill nearly 1,000 m from the onset of the Byrd flowline 160-km distant (Figure S4). Alley et al. (1997) inferred the latent heat release due to supercooling at Byrd to be three orders of magnitude lower than the geothermal flux assuming ice and water flow along a simple flowline but did not account for water concentrating along preferred pathways. Using the water routing of Le Brocq et al. (2013), based on Bedmap2 surface and bed topography (Fretwell et al., 2013), water is routed around, not up, the bedrock slopes beneath the flowline of the Byrd ice core except at more than 130 km upstream (Figure S4). Thus, conductive cooling, not hydraulic supercooling, is likely the cause of the accreted ice.

The latent heat contribution depends on the duration of freeze on, which is unknown. Gow and Meese (1996) suggest that periods of melting and freezing have alternated, implying that the geothermal flux and conductive heat flux in the basal ice are closely matched such that small variations allow a switch from freezing to melting and a long duration of net accretion. If the net accretion occurs over 50 ka, the freeze on rate is 0.1 mm/a, and the latent heat contribution of  $1 \text{ mW/m}^2$  is negligible. The average geothermal flux in the vicinity of Byrd is likely greater than the  $60 \text{ mW/m}^2$ , estimate of Rose et al.

**Table 1**  
*Geothermal Flux*

	<b>Shabtaie Ridge</b>	<b>Engelhardt Ridge</b>	<b>Roosevelt Island</b>	Siple Dome	Byrd	WAIS Divide	Grounding zone	Subglacial Lake Whillans
Constraint	<75 (9)	<85 (10)	84 (13)	71 (10)	60–75	90–260	88 (7)	285 (80)
Martos et al. (2017)	92 (12)	112 (15)	79 (11)	108 (14)	136 (22)	142 (27)	74 (12)	73 (12)
Martos minus constraint	+17	<b>+27</b>	−5	<b>+37</b>	<b>+46</b>	−	−14	<b>−212</b>
An et al. (2015)	60	66	62	65	68	68	68	66
An minus constraint	NA	NA	<b>−22</b>	−6	0	<b>−22</b>	<b>−20</b>	<b>−223</b>

Note. Bold names indicate new constraints presented in this paper. Uncertainties, if given, are in "(). "<" indicates a constraint of the maximum geothermal flux. WAIS Divide and Byrd are given as ranges. See text for explanation. Bold differences indicate exceedance of the combined uncertainty.

(1979), because 12 m/a of motion is an upper limit near the bed, and the ice flow is slower upstream; the average geothermal flux is likely less than the 75 mW/m<sup>2</sup> conducted in the ice because of the contribution of basal friction (and of basal accretion to a lesser extent). We use this range for the approximate geothermal flux at Byrd.

#### 4.2.2. WAIS Divide

At WAIS Divide, initial results (Clow et al., 2012; WDPM, 2013) suggested a high basal melt rate and thus high geothermal flux, but specific values were not published due to the large uncertainty. Significant new information was acquired after these works, including a repeat log of the borehole and the depth-age relationship in the bottom 70 m of the ice core. As part of the borehole temperature inversion, Cuffey et al. (2016) articulated that the basal melt rate can trade off with near-bed vertical strain and have little impact on the borehole temperature profile. Cuffey et al. (2016) also chose not to publish about the geothermal flux, although the analysis indicated an acceptable range of values from 90 to 260 mW/m<sup>2</sup> (Kurt Cuffey, personal communication). Thus, WAIS Divide may allow a significantly elevated geothermal flux, but the lower end of the range is within that of the Basin and Range values (Lachenbruch et al., 1994).

#### 4.3. Outlook

Despite the importance of geothermal flux to understanding the Antarctic ice sheet (Pollard et al., 2005; Seroussi et al., 2017), constraints remain sparse. Our method can be extended to other coastal domes where Raymond Arches have been imaged or can be inferred from the surface characteristics (Matsuoka et al., 2015). Coastal domes with Raymond Arches are found primarily around the edge of Antarctica and are thus good targets for investigation where the rapid flow of outlet glaciers obscures inferences of the geothermal flux. In general, coastal domes with thicker ice, lower accumulation rates, and warmer surface temperatures will provide lower estimates of the maximum geothermal flux which are the most useful. Integrating our technique with other indirect estimates (e.g., maximum geothermal fluxes from some subglacial lakes, Siegert and Dowdswell, 1996 and radar-derived estimates, Schroeder et al., 2014), the limited direct measurements, and the geologic structure (e.g., Shen et al., 2018) will allow a fuller picture of geothermal flux in Antarctica to emerge.

#### 5. Conclusion

The geothermal flux constraints from Roosevelt Island ( $84 \pm 13$  mW/m<sup>2</sup>), Engelhardt Ridge ( $<85 \pm 11$  mW/m<sup>2</sup>), and Shabtaie Ridge ( $<75 \pm 10$  mW/m<sup>2</sup>) are similar to the inferences at Siple Dome ( $71 \pm 10$  mW/m<sup>2</sup>) and Whillans grounding zone ( $88 \pm 7$  mW/m<sup>2</sup>). The remotely sensed estimates both show discrepancies from the constraints. The high heat flows of Martos et al. (2017) are not supported while the estimates of An et al. (2015) tend to be below the constraints. The geothermal flux in the deepest part of the interior (i.e., WAIS Divide) may be greater, as has also been suggested for Thwaites Glacier (Schroeder et al., 2014), but this remains unresolved. Localized high heat flow anomalies (e.g., Mt. Casertz, Blankenship et al., 1993) also exist, but the constraints suggest these are not widespread. Overall, the geothermal flux values beneath the Ross Ice Sheet are comparable to the Basin and Range in the Western United States (Lachenbruch et al., 1994).

## Data Availability Statement

Basal temperature measurements and model output will be posted to <http://www.usap-dc.org/view/project/p0000272>.

## Acknowledgments

The Washington Space Grant Summer Undergraduate Research Program and the department of Earth and Space Sciences supported SCB. We thank Taryn Black, Ed Waddington, and Howard Conway for constructive feedback and Maurice Conway, Howard Conway, Darcy Mandeno, and Hedley Berge for help with the repeat temperature measurements at Roosevelt Island. National Science Foundation Grants NSF-OPP 0943466 supported DCS and RLH and 0944307 supported TJF. We also thank ASC and the entire Roosevelt Island Climate Experiment team for their efforts in the field.

## References

- Alley, K. M., Cuffey, E. B., Evenson, J. C., Strasser, D. E. L., & Larson, G. J. (1997). How glaciers entrain and transport basal sediment: physical constraints. *Quaternary Science Reviews*, 16, 1017–1038.
- An, M. J., Wiens, D. A., Zhao, Y., Feng, M., Nyblade, A., Kanao, M., et al. (2015). Temperature, lithosphere–asthenosphere boundary, and heat flux beneath the Antarctic Plate inferred from seismic velocities. *Journal of Geophysical Research: Solid Earth*, 120, 8720–8742.
- Aydin, M., Fudge, T. J., Verhulst, K. R., Nicewonger, M. R., Waddington, E. D., & Saltzman, E. S. (2014). Carbonyl sulfide hydrolysis in Antarctic ice cores and an atmospheric history for the last 8000 years. *J. Geophys. Res. Atmos.*, 119, 8500–8514. <https://doi.org/10.1002/2014JD021618>
- Begeman, C. B., Tulaczyk, S. M., & Fisher, A. T. (2017). Spatially variable geothermal heat flux in West Antarctica: Evidence and implications. *Geophysical Research Letters*, 44, 9823–9832.
- Behrendt, J. C., Lemassurier, W. E., Cooper, A. K., Tessensohn, F., Treku, A., & Damaske, D. (1991). Geophysical studies of the West Antarctic rift system. *Tectonics*, 10(6), 1257–1273.
- Bertler, N. A. N., Conway, H., Dahl-Jensen, D., Emanuelsson, D. B., Winstrup, M., Vallelonga, P. T., et al. (2018). The Ross Sea Dipole—Temperature, snow accumulation and sea ice variability in the Ross Sea region, Antarctica, over the past 2700 years. *Climate of the Past*, 14(2), 193–214.
- Blankenship, D. D., Bell, R. E., Hodge, S. M., Brozena, J. M., Behrendt, J. C., & Finn, C. A. (1993). Active volcanism beneath the West Antarctic ice-sheet and implications for ice-sheet stability. *Nature*, 361(6412), 526–529.
- Clow, G. D., Cuffey, K. M., & Waddington, E. D. (2012). High heat-flow beneath the central portion of the West Antarctic Ice Sheet. Abstract C31A-0577 Presented at the 2012 AGU Fall Meeting, San Francisco, CA.
- Conway, H., Hall, B. L., Denton, G. H., Gades, A. M., & Waddington, E. D. (1999). Past and future grounding-line retreat of the West Antarctic Ice Sheet. *Science*, 286(5438), 280–283. <https://doi.org/10.1126/science.286.5438.280>
- Cuffey, K. M., Clow, G. D., Alley, R. B., Stuiver, M., Waddington, E. D., & Saltus, R. W. (1995). Large Arctic temperature change at the Wisconsin-Holocene glacial transition. *Science*, 270(5235), 455–458.
- Cuffey, K. M., Clow, G. D., Steig, E. J., Buizert, C., Fudge, T. J., Koutnik, M., et al. (2016). Deglacial temperature history of West Antarctica. *Proceedings of the National Academy of Sciences of the United States of America*, 113(50), 14,249–14,254. <https://doi.org/10.1073/pnas.1609132113>
- Cuffey, K. M., & Paterson, W. S. B. (2010). *Physics of Glaciers* (4th ed.). Burlington, MA: Elsevier.
- Dahl-Jensen, D., Gundestrup, N., Gogineni, S. P., & Miller, H. (2003). Basal melt at NorthGRIP modeled from borehole, ice-core and radio-echo sounder observations. *Annals of Glaciology*, 37(37), 207–212.
- Davies, J. H., & Davies, D. R. (2010). Earth's surface heat flux. *Solid Earth*, 1(1), 5–24.
- Elsberg, D. H., Harrison, W. D., Zumberge, M. A., Morack, J. L., Pettit, E. C., Waddington, E. D., & Husmann, E. (2004). Depth- and time-dependent vertical strain rates at Siple Dome, Antarctica. *Journal of Glaciology*, 50(171), 511–521.
- Engelhardt, H. (2004). Ice temperature and high geothermal flux at Siple Dome, West Antarctica, from borehole measurements. *Journal of Glaciology*, 50(169), 251–256.
- Fisher, A. T., Mankoff, K. D., Tulaczyk, S. M., Tyler, S. W., Foley, N., & Team, W. S. (2015). High geothermal heat flux measured below the West Antarctic Ice Sheet. *Science Advances*, 1(6), 9.
- Fox Maule, C., Purucker, M. E., Olsen, N., & Mosegaard, K. (2005). Heat flux anomalies in Antarctica revealed by satellite magnetic data. *Science*, 309(5733), 464–467.
- Fretwell, P., Pritchard, H. D., Vaughan, D. G., Bamber, J. L., Barrand, N. E., Bell, R., et al. (2013). Bedmap2: Improved ice bed, surface and thickness datasets for Antarctica. *Cryosphere*, 7(1), 375–393.
- Frieler, K., Clark, P. U., He, F., Buizert, C., Reese, R., Ligtenberg, S. R. M., et al. (2015). Consistent evidence of increasing Antarctic accumulation with warming. *Nature Climate Change*, 5(4), 348–352.
- Fudge, T. J., Markle, B. R., Cuffey, K. M., Buizert, C., Taylor, K. C., Steig, E. J., et al. (2016). Variable relationship between accumulation and temperature in West Antarctica for the past 31,000 years. *Geophysical Research Letters*, 43, 3795–3803.
- Gillet-Chaulet, F., Hindmarsh, R. C. A., Corr, H. F. J., King, E. C., & Jenkins, A. (2011). In-situ quantification of ice rheology and direct measurement of the Raymond Effect at Summit. *Greenland using a phase-sensitive radar*. *Geophysical Research Letters*, 38.
- Glen, J. W. (1953). RATE OF FLOW OF POLYCRYSTALLINE ICE. *Nature*, 172(4381), 721–722.
- Global Heat Flow Database (2019). [www.heatflow.und.edu/index2.html](http://www.heatflow.und.edu/index2.html)
- Golledge, N. R., Menviel, L., Carter, L., Fogwill, C. J., England, M. H., Cortese, G., & Levy, R. H. (2014). Antarctic contribution to meltwater pulse 1A from reduced Southern Ocean overturning. *Nature Communications*, 5, 5107.
- Gow, A. J., & Meese, D. E. (1996). Nature of basal debris in the GISP2 and Byrd ice cores and its relevance to bed processes. *Annals of Glaciology*, 22, 134–140.
- Gow, A. J., Ueda, H. T., & Garfield, D. E. (1968). Antarctic ice sheet—Preliminary results of first core hole to bedrock. *Science*, 161(3845), 1011–1013. <https://doi.org/10.1126/science.161.3845.1011>
- Hamilton, G. S. (2002). Mass balance and accumulation rate across Siple Dome. *West Antarctica, Annals of Glaciology*, 35, 102–106.
- Joughin, I., Tulaczyk, S., Bamber, J. L., Blankenship, D., Holt, J. W., Scambos, T., & Vaughan, D. G. (2009). Basal conditions for Pine Island and Thwaites Glaciers, West Antarctica, determined using satellite and airborne data. *Journal of Glaciology*, 55(190), 245–257.
- Joughin, I., Tulaczyk, S., MacAyeal, D. R., & Engelhardt, H. (2004). Melting and freezing beneath the Ross ice streams, Antarctica. *Journal of Glaciology*, 50(168), 96–108.
- Kingslake, J., Hindmarsh, R. C. A., Aoalgeirsdottir, G., Conway, H., Corr, H. F. J., Gillet-Chaulet, F., et al. (2014). Full-depth englacial vertical ice sheet velocities measured using phase-sensitive radar. *Journal of Geophysical Research: Earth Surface*, 119, 2604–2618.
- Lachenbruch, A. H., Sass, J. H., & Morgan, P. (1994). Thermal regime of the southern Basin and Range province: 2. Implications of heat flow for regional extension and metamorphic core complexes. *Journal of Geophysical Research*, 99(B11), 22,121–22,133.
- Le Brocq, A. M., Ross, N., Griggs, J. A., Bingham, R. G., Corr, H. F., Ferraccioli, F., et al. (2013). Evidence from ice shelves for channelized meltwater flow beneath the Antarctic Ice Sheet. *Nature Geoscience*, 6, 945–948.

- Lliboutry, L. A. (1979). A critical review of analytical approximate solutions for steady state velocities and temperatures in cold ice sheets. *Gletscherkd. Glazialgeol.*, 15, 135–148.
- MacGregor, J. A., Winebrenner, D. P., Conway, H., Matsuoka, K., Mayewski, P. A., & Clow, G. D. (2007). Modeling englacial radar attenuation at Siple Dome, West Antarctica, using ice chemistry and temperature data. *Journal of Geophysical Research*, 112, F03008.
- Martin, C., Hindmarsh, R. C. A. & Navarro, F. J. (2006). Dating ice flow change near the flow divide at Roosevelt Island, Antarctica, by using a thermomechanical model to predict radar stratigraphy, *Journal of Geophysical Research*, 111, F01011. <https://doi.org/10.1029/2005JF000326>
- Martin, C., Hindmarsh, R. C. A., & Navarro, F. J. (2009). On the effects of divide migration, along-ridge flow, and basal sliding on isochrones near an ice divide. *J. Geophys. Res.*, 114, F02006. <https://doi.org/10.1029/2008JF001025>
- Martos, Y. M., Catalan, M., Jordan, T. A., Golynsky, A., Golynsky, D., Eagles, G., & Vaughan, D. G. (2017). Heat flux distribution of Antarctica unveiled. *Geophysical Research Letters*, 44, 11417–11426.
- Matsuoka, K., Hindmarsh, R. C. A., Moholdt, G., Bentley, M. J., Pritchard, H. D., Brown, J., et al. (2015). Antarctic ice rises and ripples: Their properties and significance for ice-sheet dynamics and evolution. *Earth-Science Reviews*, 150, 724–745.
- Mulvaney, R., Triest, J., & Alemany, O. (2014). The James Ross Island and the Fletcher Promontory ice-core drilling projects. *Annals of Glaciology*, 55(68), 179–188.
- NEEM (2013). Eemian interglacial reconstructed from a Greenland folded ice core. *Nature*, 493(7433), 489–494.
- Nereson, N. A., & Raymond, C. F. (2001). The elevation history of ice streams and the spatial accumulation pattern along the Siple Coast of West Antarctica inferred from ground-based radar data from three inter-ice-stream ridges. *Journal of Glaciology*, 47(157), 303–313.
- Nereson, N. A., Raymond, C. F., Waddington, E. D., & Jacobel, R. W. (1998). Migration of the Siple Dome ice divide, West Antarctica. *Journal of Glaciology*, 44(148), 643–652.
- Pettit, E. C., Jacobson, H. P., & Waddington, E. D. (2003). Effects of basal sliding on isochrones and flow near an ice divide. *Annals of Glaciology*, 37(37), 370–376.
- Pollard, D., Deconto, R. M., & Nyblade, A. A. (2005). Sensitivity of Cenozoic Antarctic ice sheet variations to geothermal heat flux. *Global and Planetary Change*, 49, 63–74.
- Price, S. F., Conway, H., & Waddington, E. D. (2007). Evidence for late Pleistocene thinning of Siple Dome, West Antarctica. *Journal of Geophysical Research-Earth Surface*, 112(F3).
- Raymond, C. F. (1983). Deformation in the vicinity of ice divides. *Journal of Glaciology*, 29(103), 357–373.
- Rignot, E., Mouginot, J., & Scheuchl, B. (2011). Ice flow of the Antarctic ice sheet. *Science*, 333(6048), 1427–1430. <https://doi.org/10.1126/science.1208336>
- Rose, K. E. (1979). Characteristics of ice flow in Marie Byrd Land, Antarctica. *Journal of Glaciology*, 24(90), 63–75.
- Schroeder, D. M., Blankenship, D. D., Young, D. A., & Quartini, E. (2014). Evidence for elevated and spatially variable geothermal flux beneath the West Antarctic Ice Sheet. *Proceedings of the National Academy of Sciences of the United States of America*, 111(25), 9070–9072. <https://doi.org/10.1073/pnas.1405184111>
- Seroussi, H., Ivins, E. R., Wiens, D. A., & Bondzio, J. (2017). Influence of a West Antarctic mantle plume on ice sheet basal conditions. *Journal of Geophysical Research: Solid Earth*, 122, 7127–7155.
- Shapiro, N. M., & Ritzwoller, M. H. (2004). Inferring surface heat flux distributions guided by a global seismic model: Particular application to Antarctica. *Earth and Planetary Science Letters*, 223(1–2), 213–224.
- Shen, W., Wiens, D. A., Anandakrishnan, S., Aster, R. C., Gerstoft, P., Bromirski, P. D., et al. (2018). The crust and upper mantle structure of central and West Antarctica from Bayesian inversion of Rayleigh wave and receiver functions. *Journal of Geophysical Research: Solid Earth*, 123, 7824–7849. <https://doi.org/10.1029/2017JB015346>
- Siegert, M. J., & Dowdeswell, J. A. (1996). Spatial variations in heat at the base of the Antarctic ice sheet from analysis of the thermal regime above subglacial lakes. *Journal of Glaciology*, 42(142), 501–509.
- Taylor, K. C., White, J. W. C., Severinghaus, J. P., Brook, E. J., Mayewski, P. A., Alley, R. B., et al. (2004). Abrupt climate change around 22 ka on the Siple Coast of Antarctica. *Quaternary Sci. Rev.*, 23, 7–15.
- Van Ommen, T. D., Morgan, V., & Curran, M. A. J. (2004). Deglacial and holocene changes in accumulation at Law Dome, East Antarctica. *Annals of Glaciology*, 39(39), 359–365.
- Van Wyk de Vries, M., Bingham, R. G., & Hein, A. S. (2018). A new volcanic province: An inventory of subglacial volcanoes in West Antarctica, Exploration of Subsurface Antarctica: Uncovering Past Changes and Modern Processes. Geological Society, London, Special Publications, 461, 231–248. <https://doi.org/10.1144/SP461.7>
- Vaughan, D. G., Corr, H. F. J., Doake, C. S. M., & Waddington, E. D. (1999). Distortion of isochronous layers in ice revealed by ground-penetrating radar. *Nature*, 398, 323–326.
- Waddington, E. D., Conway, H., Steig, E. J., Alley, R. B., Brook, E. J., Taylor, K. C., & White, J. W. C. (2005). Decoding the dipstick: Thickness of Siple Dome, West Antarctica, at the last glacial maximum. *Geology*, 33(4), 281–284.
- White-Gaynor, A. L., Nyblade, A. A., Aster, R. C., Wiens, D. A., Bromirski, P. D., Gerstoft, P., et al. (2019). Heterogeneous upper mantle structure beneath the Ross Sea Embayment and Marie Byrd Land, West Antarctica, revealed by P-wave tomography. *Earth and Planetary Science Letters*, 513, 40–50.
- Winstrup, M., Valletlonga, P., Kjaer, H. A., Fudge, T. J., Lee, J. E., Riis, M. H., et al. (2019). A 2700-year annual timescale and accumulation history for an ice core from Roosevelt Island, West Antarctica. *Climate of the Past*, 15(2), 751–779.